



Bis(mefloquinium) butanedioate ethanol monosolvate: crystal structure and Hirshfeld surface analysis

James L. Wardell, Mukesh M. Jotani and Edward R. T. Tiekink

Acta Cryst. (2019). **E75**, 1162–1168



IUCr Journals

CRYSTALLOGRAPHY JOURNALS ONLINE

This open-access article is distributed under the terms of the Creative Commons Attribution Licence <http://creativecommons.org/licenses/by/4.0/legalcode>, which permits unrestricted use, distribution, and reproduction in any medium, provided the original authors and source are cited.



Received 3 July 2019
Accepted 6 July 2019

Edited by W. T. A. Harrison, University of Aberdeen, Scotland

‡ Additional correspondence author, e-mail: j.wardell@abdn.ac.uk.

Keywords: crystal structure; mefloquine; salt; hydrogen bonding; Hirshfeld surface analysis.

CCDC reference: 1938793

Supporting information: this article has supporting information at journals.iucr.org/e

Bis(mefloquinium) butanedioate ethanol monosolvate: crystal structure and Hirshfeld surface analysis

James L. Wardell,^a‡ Mukesh M. Jotani^b and Edward R. T. Tiekkink^c*

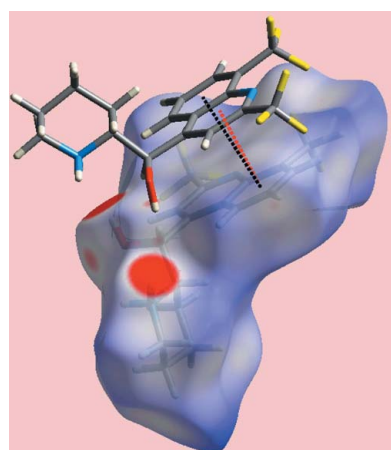
^aFundação Oswaldo Cruz, Instituto de Tecnologia em Fármacos-Far Manguinhos, 21041-250 Rio de Janeiro, RJ, Brazil,

^bDepartment of Physics, Bhavan's Sheth R. A. College of Science, Ahmedabad, Gujarat 380001, India, and ^cResearch Centre for Crystalline Materials, School of Science and Technology, Sunway University, 47500 Bandar Sunway, Selangor Darul Ehsan, Malaysia. *Correspondence e-mail: edwardt@sunway.edu.my

The asymmetric unit of the centrosymmetric title salt solvate, $2\text{C}_{17}\text{H}_{17}\text{F}_6\text{N}_2\text{O}^+ \cdot \text{C}_4\text{H}_4\text{O}_4^{2-} \cdot \text{CH}_3\text{CH}_2\text{OH}$, (systematic name: 2-{{[2,8-bis(trifluoromethyl)quinolin-4-yl]hydroxymethyl}piperidin-1-ium butanedioate ethanol monosolvate) comprises two independent cations, with almost superimposable conformations and each approximating the shape of the letter *L*, a butanedioate dianion with an all-*trans* conformation and an ethanol solvent molecule. In the crystal, supramolecular chains along the *a*-axis direction are sustained by charge-assisted hydroxy-O—H···O(carboxylate) and ammonium-N—H···O(carboxylate) hydrogen bonds. These are connected into a layer via C—F···π(pyridyl) contacts and π—π stacking interactions between quinolinyl-C₆ and —NC₅ rings of the independent cations of the asymmetric unit [inter-centroid separations = 3.6784 (17) and 3.6866 (17) Å]. Layers stack along the *c*-axis direction with no directional interactions between them. The analysis of the calculated Hirshfeld surface reveals the significance of the fluorine atoms in surface contacts. Thus, by far the greatest contribution to the surface contacts, *i.e.* 41.2%, are of the type F···H/H···F and many of these occur in the inter-layer region. However, these contacts occur at separations beyond the sum of the van der Waals radii for these atoms. It is noted that H···H contacts contribute 29.8% to the overall surface, with smaller contributions from O···H/H···O (14.0%) and F···F (5.7%) contacts.

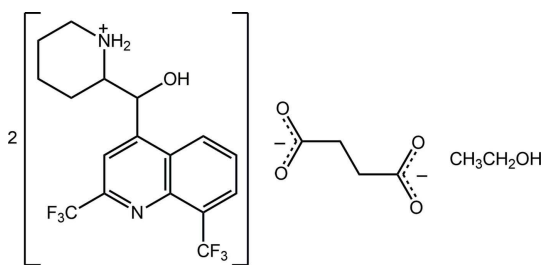
1. Chemical context

Malaria continues to be a major worldwide health issue and vast populations in tropical countries, including visitors to those regions, are susceptible to the disease, which is spread by parasites such as *Plasmodium falciparum* (Maguire *et al.*, 2006). The problem is compounded by the parasites' abilities to develop resistance to drugs, such as to the once popular chloroquine (Grabias & Kumar, 2016). Mefloquine, [2,8-bis(trifluoromethyl)quinolin-4-yl]-piperidin-2-ylmethanol, is a drug used against malaria (Tickell-Painter *et al.*, 2017). The molecule contains two adjacent chiral centres, *i.e.* one at the carbon atom carrying the hydroxy group and one at the link connecting the piperidinyl ring to the rest of the molecule. The drug is commonly marketed as *Lariam*, which is the hydrochloride salt, comprising (R*,S*)-(2-{{[2,8-bis(trifluoromethyl)quinolin-4-yl]hydroxymethyl}piperidin-1-ium chloride and its (S*,R*) enantiomer. While the former is effective against malaria, the latter has an affinity for the adenosine acceptors in the brain, inducing serious psychiatric and neurologic side-effects (Nevin, 2017). Hence, experiments at resolving the



OPEN ACCESS

enantiomers are of practical importance (Engwerda *et al.*, 2019). Herein, as continuation of our anion-exchange experiments of the racemic salt and attendant structural studies (Wardell *et al.*, 2016; Wardell, Wardell *et al.*, 2018; Wardell, Jotani *et al.*, 2018; Wardell & Tiekkink, 2019), the crystal and molecular structures of the butanedioate salt, isolated as an ethanol monosolvate, are described along with an analysis of the calculated Hirshfeld surfaces.



2. Structural commentary

The asymmetric unit of the salt solvate, (I), comprises two mefloquinium cations, a butanedioate dianion and a solvent ethanol molecule; the molecular structures of the ions are shown in Fig. 1. Evidence of proton transfer during crystallization is seen in the relatively small difference in the C \cdots O bond lengths of the dianion, *i.e.* C35—O3, O4 = 1.236 (4) and 1.285 (3) Å, and C38—O5, O6 = 1.255 (4) and 1.271 (4) Å. While normally these bond lengths might be expected to be closer to equivalent, as noted below, each of the O4 and O6 atoms participate in two strong charge-assisted hydrogen bonds, see *Supramolecular features*, which explains the slightly longer C \cdots O bond lengths formed by these atoms. Further support for proton transfer leading to the formation of piperidin-1-ium cations is supported by the pattern of hydrogen bonding involving the ammonium-N—H hydrogen atoms, as discussed below in *Supramolecular features*.

The cations exhibit very similar molecular geometries, as highlighted in the overlay diagram of Fig. 2. There are two chiral centres in each cation and the illustrated cations are *R* at C12 and *S* at C13 for the N1-cation, and *R* at C29 and *S* at C30 for the N3-cation, *i.e.* each conforms to the [(+)-*erythro*-

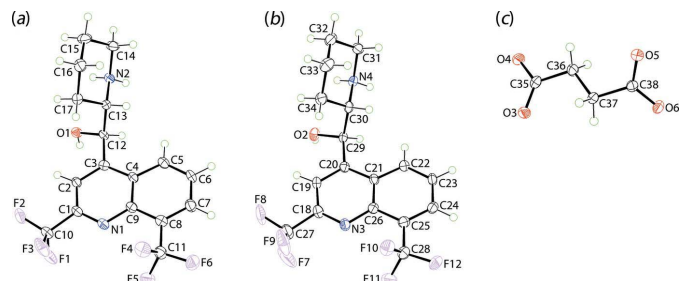


Figure 1

The molecular structures of the ionic components of the asymmetric unit of (I) showing the atom-labelling scheme and displacement ellipsoids at the 50% probability level: (a) the N1-containing cation, (b) the N3-cation and (c) the butanedioate dianion.

Table 1
Hydrogen-bond geometry (Å, °).

Cg1 is the centroid of the (N1,C1—C4,C9) ring.

D—H \cdots A	D—H	H \cdots A	D \cdots A	D—H \cdots A
N2—H1N \cdots O1	0.88 (3)	2.49 (3)	2.806 (4)	102 (2)
N4—H3N \cdots O2	0.88 (2)	2.54 (3)	2.863 (4)	103 (2)
O1—H1O \cdots O6	0.84 (3)	1.81 (3)	2.653 (3)	175 (2)
O2—H2O \cdots O4 ⁱ	0.84 (2)	1.82 (2)	2.656 (3)	170 (3)
N2—H1N \cdots O5 ⁱⁱ	0.88 (3)	1.97 (3)	2.830 (4)	165 (3)
N2—H2N \cdots O4 ⁱⁱ	0.88 (3)	1.82 (3)	2.694 (4)	173 (3)
N4—H3N \cdots O3 ⁱⁱ	0.88 (2)	1.99 (3)	2.832 (4)	161 (3)
N4—H4N \cdots O6	0.89 (3)	1.92 (3)	2.789 (4)	168 (3)
O7—H7O \cdots O5	0.85 (3)	1.88 (3)	2.729 (4)	176 (7)
C30—H30 \cdots O7	1.00	2.40	3.296 (4)	149
C10—F3 \cdots Cg1 ⁱⁱⁱ	1.32 (1)	3.28 (1)	4.101 (3)	120 (1)

Symmetry codes: (i) $x - 1, y, z$; (ii) $-x, -y + 2, -z$; (iii) $-x, -y + 1, -z$.

mefloquinium] isomer; space-group symmetry indicates that the unit cell contains equal numbers of both enantiomers. The r.m.s. deviation for the ten atoms comprising the N1-quinolinyl residue is 0.0254 Å [0.0256 Å for the N3-quinolinyl residue], with the hydroxyl-O1 and ammonium-N2 atoms lying to either side of the plane, *i.e.* $-0.323 (4)$ and $1.302 (6)$ Å, respectively [0.255 (4) Å for O2 and $-1.348 (6)$ Å for N4]. The dihedral angle of $72.55 (9)^\circ$ [$71.48 (9)^\circ$] formed between the fused ring system and the least-squares plane through the piperinium ring indicates that, to a first approximation, the molecule has the shape of the letter *L*. Referring to Table 1, an intramolecular charge-assisted ammonium-N $^+$ —H \cdots O(hydroxy) hydrogen-bond is formed as the hydroxyl-O1 and ammonium-N2 atoms lie to the same side of the cation with

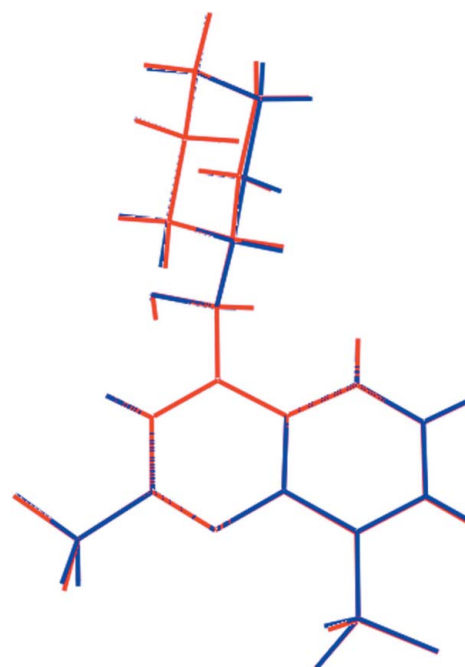


Figure 2

An overlay diagram of the N1- (red image) and N3-containing cations. The cations have been superimposed so that the C₅N rings of the quinolinyl residues are coincident.

the O1—C12—C13—N2 torsion angle of $-63.4(3)^\circ$ indicating a + syn-clinal relationship [O2—C29—C30—N4 = $-68.4(3)^\circ$].

In the butanedioate dianion, the C35—C36—C38—C39 torsion angle of $175.4(3)^\circ$ indicates an all-*trans* conformation (+ anti-periplanar). The dihedral angle formed between the terminal carboxylate residues is $51.0(2)^\circ$, indicating that the dianion is considerably twisted.

3. Supramolecular features

The most prominent feature of the molecular packing is the formation of twisted supramolecular chains propagating parallel to the *a*-axis direction, Table 1 and Fig. 3*a*. Each of the cation-bound hydroxy groups forms a charge-assisted hydroxy-O—H···O(carboxylate) hydrogen bond to a carboxylate-O atom, at opposite ends of the butanedioate dianion. In addition, each of the four ammonium-N—H hydrogen atoms connects to a carboxylate-O atom, each derived from a different carboxylate residue, *via* a charge-assisted ammonium-N—H···O(carboxylate) hydrogen bond. Thus, each of

the O4 and O6 atoms accept two charge-assisted hydrogen bonds. The carboxylate-O5 atom accepts a hydrogen bond from the solvent ethanol molecule, while ethanol-O7 participates in a methine-C—H···O interaction, Table 1. The carboxylate-O3 atom forms only one hydrogen bond. The number and strength of hydrogen bonds formed by the carboxylate-O atoms correlates with the magnitude of the C—O bond lengths, *e.g.* the C35—O3 < C38—O5 < C38—O6 < C35—O4 (see comment in *Structural Commentary*).

The connections between the chains leading to supramolecular layers that stack along the *c*-axis direction are of the type C—F···π(pyridyl), Table 1, occurring between N1-containing cations, and π—π stacking interactions between the independent molecules comprising the asymmetric unit. The latter occur between the C₆ ring of the N1-quinolinyl residue (C4—C9) and each of the N3-quinolinyl-bound pyridyl (N3,C18—C21,C26) [inter-centroid separation = $3.6784(17)$ Å, angle of inclination = $4.27(14)^\circ$] and C₆ (C21—C26) [$3.6866(17)$ Å, angle of inclination = $3.67(14)^\circ$] rings. A view of the unit-cell contents is shown in Fig. 3*b*.

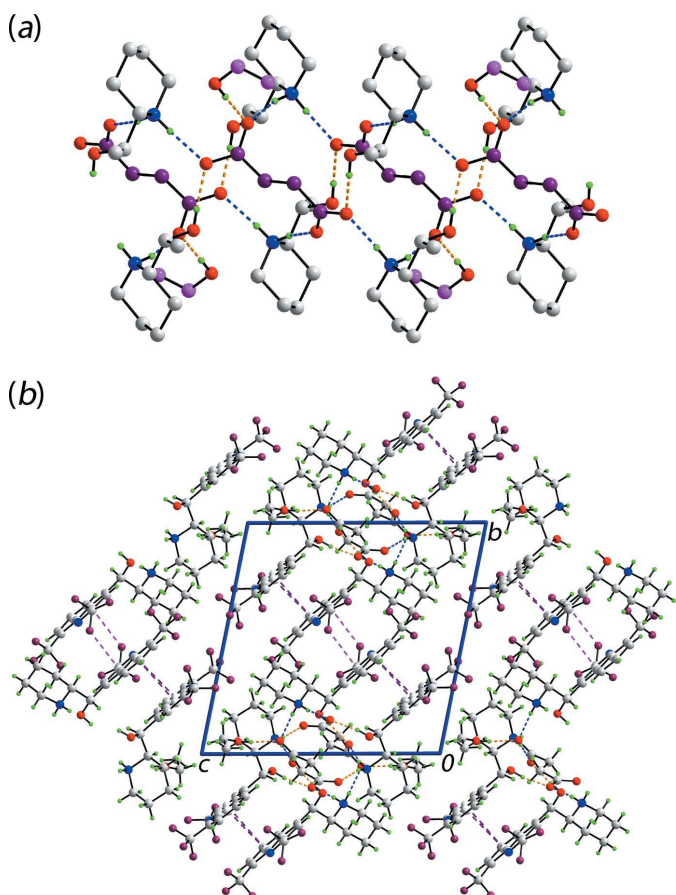


Figure 3

Molecular packing in (I): (a) The supramolecular chain along the *a* axis, being sustained by O—H···O (orange dashed lines) and N—H···O (blue dashed lines) hydrogen bonding with non-participating H atoms omitted and (b) a view of the unit-cell contents shown in projection down the *a* axis, the axis of propagation of the chain shown in (a). The C—Cl···π and C—F···π interactions are shown as pink and purple dashed lines, respectively.

4. Hirshfeld surface analysis

The analysis of Hirshfeld surface calculations for (I) was performed in order to learn more about the supramolecular association, in particular, about the inter-layer connections, following established procedures (Tan *et al.*, 2019) and employing *Crystal Explorer* 17 (Turner *et al.*, 2017). Such analyses have proven useful for salts with multiple components comprising the asymmetric unit (Jotani *et al.*, 2019).

It is clearly evident from the numerous characteristic red spots on the Hirshfeld surfaces mapped over *d*_{norm} for the constituents of (I), shown in Fig. 4, that the butanedioate dianion plays a crucial role in forming significant interactions with each of the two independent mefloquine cations as well as with the ethanol solvent molecule. The O—H···O and N—H···O hydrogen bonds summarized in Table 1 are characterized as bright-red spots on the Hirshfeld surface mapped over *d*_{norm} for the dianion, Fig. 4*a* and *b*, and near the

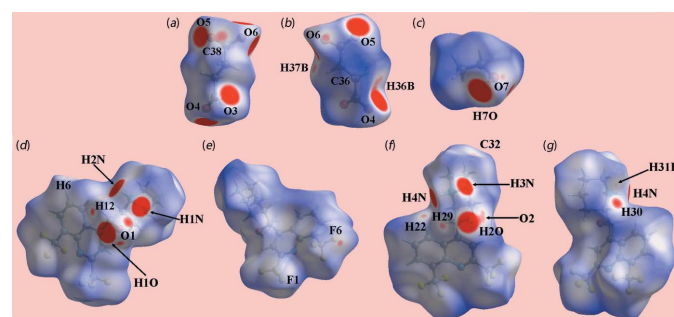


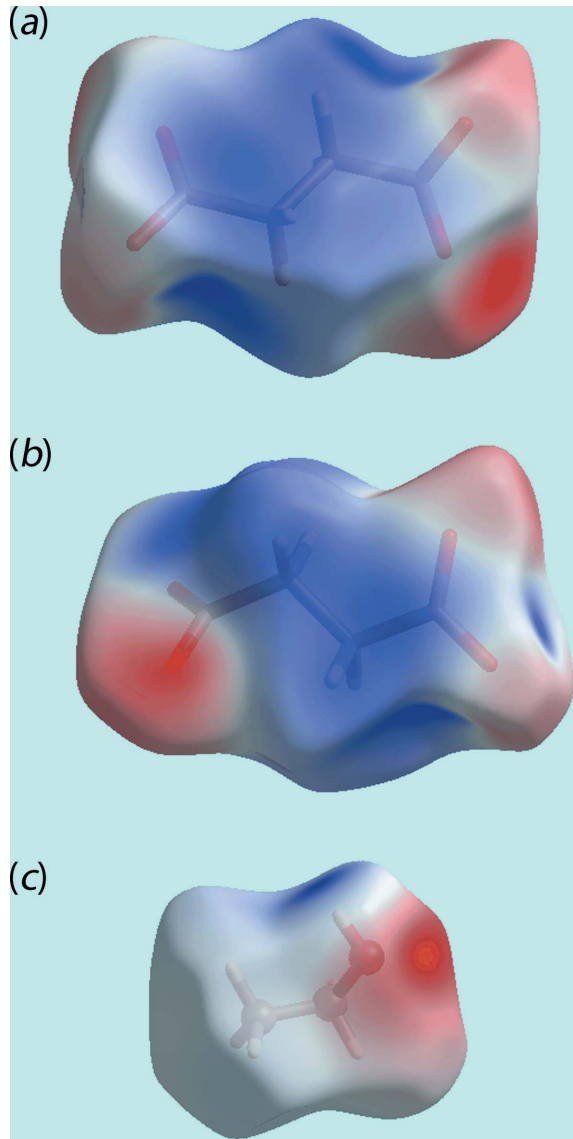
Figure 4

Views of the Hirshfeld surface of (I) mapped over *d*_{norm} for the: (a) and (b) dianion in the range -0.229 to $+1.450$ arbitrary units (a.u.), (c) ethanol molecule (-0.169 to $+1.471$ a.u.), (d) and (e) O1-containing cation (-0.229 to $+2.242$ a.u.) and (f) and (g) O2-containing cation (-0.219 to $+2.159$ a.u.).

Table 2Summary of short interatomic contacts (\AA) in (I)^a.

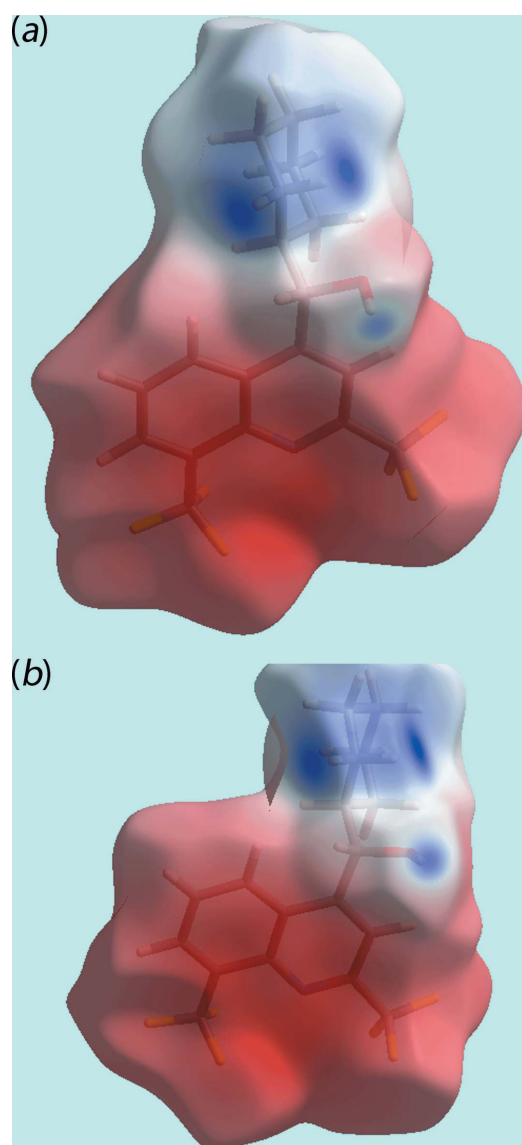
Contact	Distance	Symmetry operation
F1···H6	2.50	$1 + x, y, z$
F6···C32	3.096 (4)	$x, -1 + y, z$
O1···H37B	2.45	x, y, z
O1···C38	3.038 (4)	$-x, -y, -1 - z$
O2···H36B	2.50	$-1 + x, y, z$
O2···C36	3.090 (4)	$-1 + x, y, z$
O4···H12	2.53	$1 + x, y, z$
O6···H22	2.50	x, y, z
O7···H31B	2.55	x, y, z
H1O···H37B	2.14	x, y, z
H12···H29	2.06	x, y, z
H34A···H39A	2.22	$-x, 2 - y, -z$

Notes: (a) The interatomic distances are calculated in *Crystal Explorer* (Turner *et al.*, 2017) whereby the $X\text{--H}$ bond lengths are adjusted to their neutron values.

**Figure 5**

Views of Hirshfeld surface mapped over electrostatic potential for the: (a) and (b) dianion in the range -0.072 to $+0.066$ atomic units (au) and (c) ethanol molecule (-0.077 to $+0.159$ au). The red and blue regions represent negative and positive electrostatic potentials, respectively.

respective donors on the Hirshfeld surfaces of the ethanol molecule, Fig. 4c, and melfloquinium cations in Fig. 4d and e. The effects of the short inter-atomic contacts on the packing of (I), summarized in Table 2, are also evident as the faint-red spots near the respective atoms, Fig. 4. The blue and red regions corresponding to positive and negative potentials, respectively, around the atoms of the dianion and solvent ethanol molecule, Fig. 5, and cations, Fig. 6, on the Hirshfeld surfaces mapped over electrostatic potential also represent donors and acceptors of the respective hydrogen bonds. The additional influence of the C–F··· π contacts involving the F2 and F3 atoms interacting with the (C4–C9) and N1-pyridyl rings of the N1-quinolinyl residue are viewed as blue bumps and bright-orange concave regions, respectively, on the

**Figure 6**

Views of Hirshfeld surface mapped over electrostatic potential for the: (a) O1-containing cation in the range -0.262 to $+0.215$ atomic units (au) and (b) O2-containing cation (-0.255 to $+0.198$ au). The red and blue regions represent negative and positive electrostatic potentials, respectively.

Table 3
Percentage contributions of interatomic contacts to the Hirshfeld surface for (I).

Contact	Percentage contribution
H···H	29.8
O···H/H···O	14.0
F···H/H···F	41.2
F···F	5.7
C···H/H···C	4.1
C···F/F···C	2.8
N···H/H···N	1.0
C···N/N···C	0.5
C···O/O···C	0.3
O···O	0.2
F···N/N···F	0.2
C···C	0.2
F···O/O···F	0.1

Hirshfeld surface mapped with the shape-index property in Fig. 7. The π – π contacts formed between the (C4–C9) ring of the O1-cation and each of the (C21–C26) and N3-pyridyl rings of the O2-cation are illustrated in Fig. 8.

The overall two-dimensional fingerprint plot for (I), Fig. 9a, and those delineated into specific H···H, O···H/H···O, F···H/H···F, C···F/F···C and C···O/O···C contacts (McKinnon *et al.*, 2007) are illustrated in Fig. 9b–e; the percentage contributions from the different inter-atomic contacts to the Hirshfeld surface are summarized in Table 3. The relatively small percentage contribution from H···H contacts to the Hirshfeld surface in the overall packing of (I) is due to the formation of a wide range of different intermolecular interactions between the constituent cations, dianions and solvent ethanol molecule. This is well-evidenced in the long list of contacts in Table 3. The presence of two trifluoromethyl groups in each of the independent cations results in a major contribution from fluorine atoms to the Hirshfeld surface of (I), as highlighted in Table 3. Indeed, the major contributor of contacts to the surface is of the type F···H/H···F, at 41.2%. Many of these occur in the inter-layer

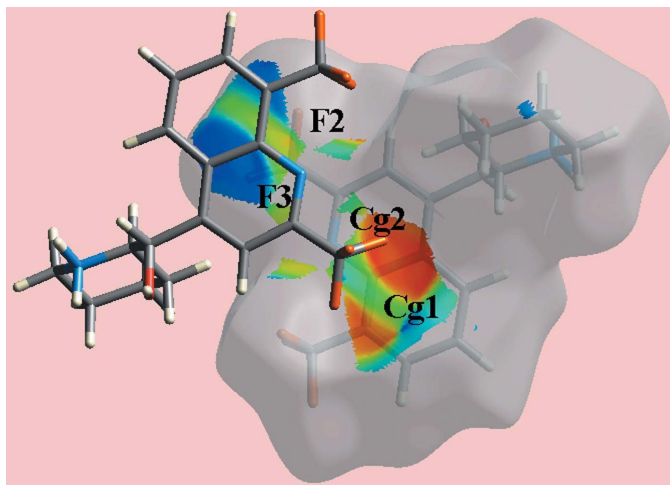


Figure 7

A view of Hirshfeld surface mapped over the shape-index property highlighting the intermolecular C–F···π/π···F–C contacts by blue bumps and bright-orange concave regions.

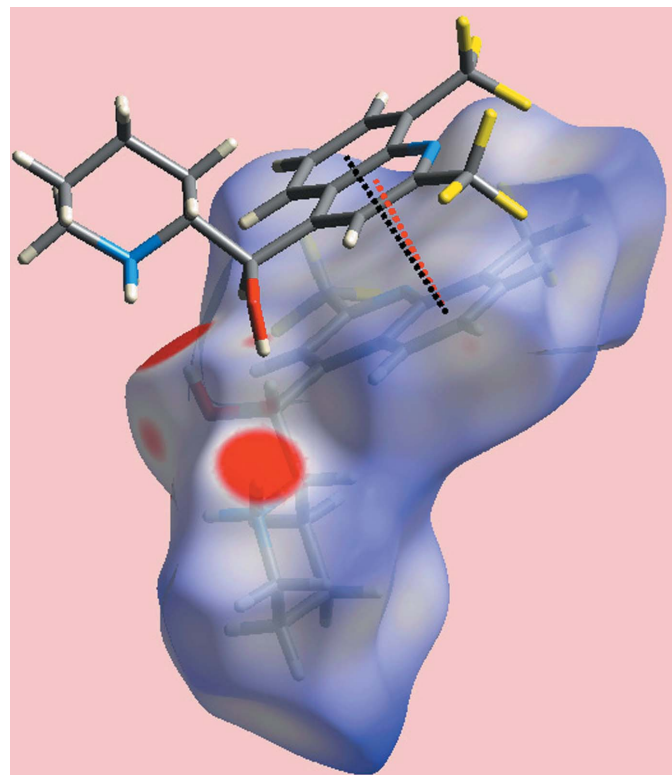
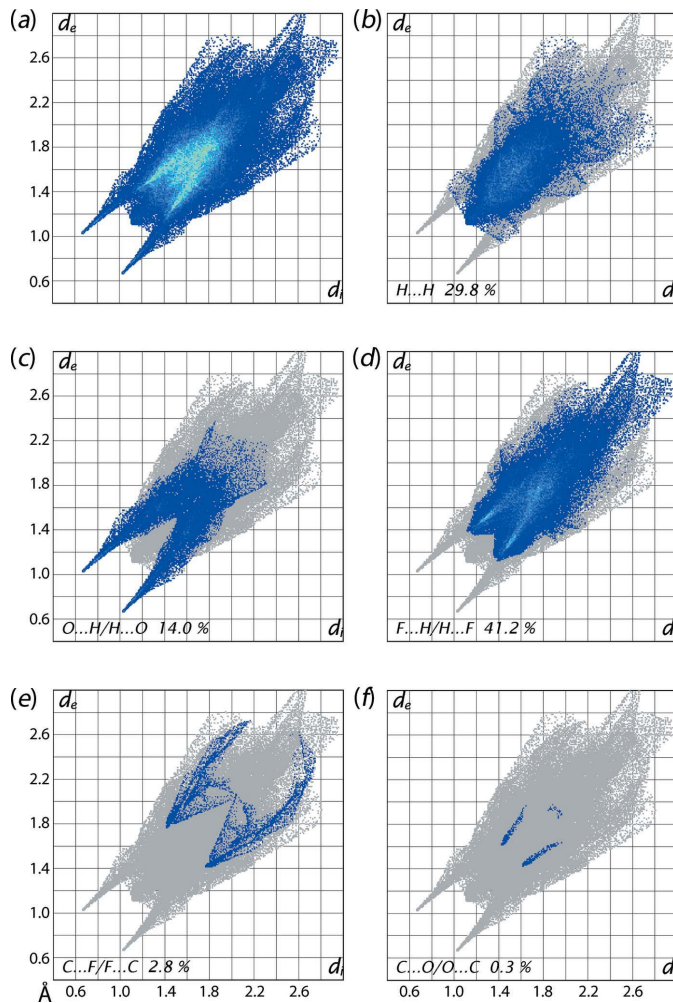


Figure 8

A view of Hirshfeld surface mapped over d_{norm} for the O1-containing cation in the range –0.229 to + 2.242 arbitrary units highlighting the intramolecular π – π contacts between the (C4–C9) ring of the O1-containing cation and the (C21–C26) and N3-pyridyl rings of the O2-containing cation by red and black dotted lines, respectively.

region at separations greater than the sum of the van der Waals radii.

The presence of a cone-shaped tip at $d_e + d_i \sim 2.2 \text{ \AA}$ in the fingerprint plot delineated into H···H contacts in Fig. 9b, is an indication of the short interatomic H···H contact between symmetry-related piperidinium-H34A and ethanol-H39A atoms, Table 2. The other short H···H contacts summarized in Table 2 occur between the hydrogen atoms of the cations and dianion within the asymmetric unit. In the fingerprint plot delineated into O···H/H···O contacts, Fig. 9c, the pair of long spikes with their tips at $d_e + d_i \sim 1.8 \text{ \AA}$ are due to the O–H···O and N–H···O hydrogen bonds involving the carboxylate-O4 atom of the dianion whereas the points corresponding to N–H···O hydrogen bonds involving the O3 and O5 atoms of the dianion and those involved in short interatomic O···H contacts, Table 2, are merged within the plot. The pair of conical tips at $d_e + d_i \sim 2.5 \text{ \AA}$ in the fingerprint plot delineated into F···H/H···F contacts, Fig. 9d, represent the presence of these short contacts. The effect of intermolecular C–F···π/π···F–C and short interatomic C···F/F···C contacts on the molecular packing, Table 3, results in a small but measurable contribution of 2.8% to the Hirshfeld surface of (I) and are viewed as the pair of forceps-like tips at $d_e + d_i \sim 3.1 \text{ \AA}$ in Fig. 9e. The presence of short interatomic C···O/O···C contacts involving the hydroxyl-O1 and -O2 atoms are characterized as a pair of leaf-like tips at $d_e + d_i$

**Figure 9**

(a) The full two-dimensional fingerprint plot for (I) and (b)–(f) those delineated into H···H, O···H/H···O, F···H/H···F, C···F/F···C and C···O/O···C contacts, respectively.

~3.0 Å in Fig. 9f. Finally, the presence of π – π stacking interactions between the (C4–C9) ring of the O1-cation and the (C21–C26) and N3-pyridyl rings of the O2-cation are reflected in the 3.4 and 3.3% contributions from C···C contacts to the Hirshfeld surfaces of the individual cations; although the contribution from these contacts to the surfaces in the overall structure of (I) is negligible as these are embedded within the asymmetric unit.

5. Database survey

As indicated in the *Chemical context*, the specific enantiomer of *Lariam* is important in terms of pharmacological activity. Hence, considerable investment has been made in attempting to resolve the enantiomers by salt formation. During such studies, a seemingly high propensity towards kryptoracemic behaviour has been revealed. Kryptoracemic behaviour is related to the rare phenomenon where enantiomeric molecules crystallize in one of the 65 Sohncke space groups, *i.e.* space groups which lack an inversion centre, a rotatory

inversion axis, a glide plane or a mirror plane. In these circumstances, the enantiomeric molecules are related by non-crystallographic symmetry, *e.g.* a non-crystallographic centre of inversion. A review of this phenomenon has appeared for organic compounds (Fábián & Brock, 2010) where such behaviour is found in only 0.1% of structures. There are about 30 mefloquine/derivatives in the Cambridge Structural Database (Groom *et al.*, 2016) and of these, there are two examples of kryptoracemates (Jotani *et al.*, 2016; Wardell, Wardell *et al.*, 2016). Further, in a very recent study, 34 new mefloquine salts were reported of which two were kryptoracemates (Engwerda *et al.*, 2019). Such a high adoption of kryptoracemic behaviour by these species suggest that further, systematic structural studies are warranted.

6. Synthesis and crystallization

A solution of mefloquinium chloride (1 mmol) and sodium succinate (2 mmol) in ethanol (15 ml) was refluxed for 30 min. The reaction mixture was left at room temperature and after three days, colourless platy crystals of (I) were collected; m.p. 505–505 K. Yield of recrystallized product 65%.

^1H NMR (DMSO- d_6): δ : 1.15–1.27 (2H, *m*), 1.32–1.47 (6H, *m*), 1.48–1.57 (2H, *br. d*), 1.65–1.74 (2H, *br. d*), 2.33 (4H, *s*; succinate), 2.58–2.67 (2H, *br. t*), 3.00–3.11 (4H, *m*), 5.58 (2H, *d*, J = 8 Hz), 7.95 (2H, *t*, J = 8 Hz), 8.10 (2H, *s*), 8.37 (2H, *t*, J = 7.2 Hz), 8.75 (2H, *d*, J = 8 Hz), resonances due to OH and NH were not observed. Resonances due to ethanol solvate were also present: 3.45 (*q*, J = 7.0 Hz) and 1.07 (*t*, J = 7.0 Hz). ^{13}C NMR (DMSO- d_6): δ : 22.92, 24.28, 24.71, 31.76, 45.55, 60.57, 70.33, 115.58, 119.89 ($J_{\text{C},\text{F}}$ = 273.8 Hz), 122.34, 122.64 ($J_{\text{C},\text{F}}$ = 271.7 Hz), 127.77 ($J_{\text{C},\text{F}}$ = 29.0 Hz), 127.76, 129.40, 129.9 ($J_{\text{C},\text{F}}$ = 5.2 Hz), 142.74, 146.56 ($J_{\text{C},\text{F}}$ = 34.5 Hz), 153.13, 175.32). ^{19}F NMR (DMSO- d_6): δ : –58.83, –66.63. IR (cm^{-1}) 3500–2100 (*br*), 1589 (*br*), 1514, 1454, 1430, 1371, 1312, 1267, 1217, 1182, 1111, 1053, 1018, 986, 941, 910, 837, 777, 546, 445.

7. Refinement

Crystal data, data collection and structure refinement details are summarized in Table 4. The carbon-bound H atoms were placed in calculated positions ($\text{C}–\text{H}$ = 0.95–1.00 Å) and were included in the refinement in the riding-model approximation, with $U_{\text{iso}}(\text{H})$ set to 1.2–1.5 $U_{\text{eq}}(\text{C})$. The O- and N-bound H atoms were refined with distance restraints 0.84 ± 0.01 and 0.88 ± 0.01 Å, respectively, and refined with $U_{\text{iso}}(\text{H})$ = 1.5 $U_{\text{eq}}(\text{O})$ and 1.2 $U_{\text{eq}}(\text{N})$, respectively. Owing to poor agreement, the (012) reflection was omitted from the final cycles of refinement.

Acknowledgements

The use of the EPSRC X-ray crystallographic service at the University of Southampton, England, and the valuable assistance of the staff there is gratefully acknowledged. JLW acknowledges support from CNPq (Brazil).

Funding information

Sunway University Sdn Bhd (grant. No. STR-RCTR-RCCM-001–2019) is thanked for financial support of this work.

References

- Brandenburg, K. (2006). *DIAMOND*. Crystal Impact GbR, Bonn, Germany.
- Engwerda, A. H. J., Maassen, R., Tinnemans, P., Meekes, H., Rutjes, F. P. J. T. & Vlieg, E. (2019). *Angew. Chem. Int. Ed.* **58**, 1670–1673.
- Fábián, L. & Brock, C. P. (2010). *Acta Cryst. B* **66**, 94–103.
- Farrugia, L. J. (2012). *J. Appl. Cryst.* **45**, 849–854.
- Grabias, B. & Kumar, S. (2016). *Expert Opin. Drug Saf.* **15**, 903–910.
- Groom, C. R., Bruno, I. J., Lightfoot, M. P. & Ward, S. C. (2016). *Acta Cryst. B* **72**, 171–179.
- Hooft, R. W. W. (1998). *COLLECT*. Nonius BV, Delft, The Netherlands.
- Jotani, M. M., Wardell, J. L. & Tiekkink, E. R. T. (2016). *Z. Kristallogr.* **231**, 247–255.
- Jotani, M. M., Wardell, J. L. & Tiekkink, E. R. T. (2019). *Z. Kristallogr. Cryst. Mater.* **234**, 43–57.
- Maguire, J. D., Krisin Marwoto, H., Richie, T. L., Fryauff, D. J. & Baird, J. K. (2006). *Clin. Infect. Dis.* **42**, 1067–1072.
- McKinnon, J. J., Jayatilaka, D. & Spackman, M. A. (2007). *Chem. Commun.* pp. 3814–3816.
- Nevin, R. L. (2017). *Pharmacol. Res.* pp. 5, article No. e00328.
- Otwinowski, Z. & Minor, W. (1997). *Methods in Enzymology*, Vol. 276, *Macromolecular Crystallography*, Part A, edited by C. W. Carter Jr & R. M. Sweet, pp. 307–326. New York: Academic Press.
- Sheldrick, G. M. (2007). *SADABS*. Bruker AXS Inc., Madison, Wisconsin, USA.
- Sheldrick, G. M. (2008). *Acta Cryst. A* **64**, 112–122.
- Sheldrick, G. M. (2015). *Acta Cryst. C* **71**, 3–8.
- Tan, S. L., Jotani, M. M. & Tiekkink, E. R. T. (2019). *Acta Cryst. E* **75**, 308–318.
- Tickell-Painter, M., Maayan, N., Saunders, R., Pace, C. & Sinclair, D. (2017). *Cochrane Database Syst. Rev.* 10 art. no. CD006491.
- Turner, M. J., McKinnon, J. J., Wolff, S. K., Grimwood, D. J., Spackman, P. R., Jayatilaka, D. & Spackman, M. A. (2017). *Crystal Explorer 17*. The University of Western Australia.
- Wardell, J. L., Jotani, M. M. & Tiekkink, E. R. T. (2016). *Acta Cryst. E* **72**, 1618–1627.
- Wardell, J. L., Jotani, M. M. & Tiekkink, E. R. T. (2018). *Acta Cryst. E* **74**, 1851–1856.

Table 4
Experimental details.

Crystal data	
Chemical formula	$2\text{C}_{17}\text{H}_{17}\text{F}_6\text{N}_2\text{O}^+\cdot\text{C}_4\text{H}_4\text{O}_4^{2-}\cdot\text{C}_2\text{H}_6\text{O}$
M_r	920.79
Crystal system, space group	Triclinic, $P\bar{1}$
Temperature (K)	120
a, b, c (Å)	10.0405 (2), 14.6482 (4), 14.6547 (4)
α, β, γ (°)	100.745 (1), 93.830 (2), 98.497 (2)
V (Å ³)	2084.41 (9)
Z	2
Radiation type	Mo $K\alpha$
μ (mm ⁻¹)	0.14
Crystal size (mm)	0.42 × 0.05 × 0.03
Data collection	
Diffractometer	Bruker–Nonius Roper CCD camera on κ -goniostat
Absorption correction	Multi-scan (<i>SADABS</i> ; Sheldrick, 2007)
T_{\min}, T_{\max}	0.849, 1.000
No. of measured, independent and observed [$I > 2\sigma(I)$] reflections	42885, 9543, 6505
R_{int}	0.085
(sin θ/λ) _{max} (Å ⁻¹)	0.651
Refinement	
$R[F^2 > 2\sigma(F^2)]$, $wR(F^2)$, S	0.074, 0.180, 1.04
No. of reflections	9543
No. of parameters	590
No. of restraints	7
H-atom treatment	H atoms treated by a mixture of independent and constrained refinement
$\Delta\rho_{\text{max}}, \Delta\rho_{\text{min}}$ (e Å ⁻³)	0.60, -0.58

Computer programs: *DENZO* (Otwinowski & Minor, 1997) and *COLLECT* (Hooft, 1998), *SHELXS97* (Sheldrick, 2008), *SHELXL2014* (Sheldrick, 2015), *ORTEP-3 for Windows* (Farrugia, 2012), *DIAMOND* (Brandenburg, 2006) and *publCIF* (Westrip, 2010).

- Wardell, J. L. & Tiekkink, E. R. T. (2019). *Z. Kristallogr. New Cryst. Struct.* **234**, 687–689.
- Wardell, J. L., Wardell, S. M. S. V., Jotani, M. M. & Tiekkink, E. R. T. (2018). *Acta Cryst. E* **74**, 895–900.
- Westrip, S. P. (2010). *J. Appl. Cryst.* **43**, 920–925.

supporting information

Acta Cryst. (2019). E75, 1162-1168 [https://doi.org/10.1107/S2056989019009654]

Bis(mefloquinium) butanedioate ethanol monosolvate: crystal structure and Hirshfeld surface analysis

James L. Wardell, Mukesh M. Jotani and Edward R. T. Tieckink

Computing details

Data collection: *COLLECT* (Hooft, 1998); cell refinement: *DENZO* (Otwinowski & Minor, 1997) and *COLLECT* (Hooft, 1998); data reduction: *DENZO* (Otwinowski & Minor, 1997) and *COLLECT* (Hooft, 1998); program(s) used to solve structure: *SHELXS97* (Sheldrick, 2008); program(s) used to refine structure: *SHELXL2014* (Sheldrick, 2015); molecular graphics: *ORTEP-3 for Windows* (Farrugia, 2012) and *DIAMOND* (Brandenburg, 2006); software used to prepare material for publication: *publCIF* (Westrip, 2010).

2-{[2,8-Bis(trifluoromethyl)quinolin-4-yl](hydroxy)methyl}piperidin-1-ium butanedioate ethanol monosolvate

Crystal data

$2\text{C}_{17}\text{H}_{17}\text{F}_6\text{N}_2\text{O}^+\cdot\text{C}_4\text{H}_4\text{O}_4^{2-}\cdot\text{C}_2\text{H}_6\text{O}$	$Z = 2$
$M_r = 920.79$	$F(000) = 952$
Triclinic, $P\bar{1}$	$D_x = 1.467 \text{ Mg m}^{-3}$
$a = 10.0405 (2) \text{ \AA}$	Mo $K\alpha$ radiation, $\lambda = 0.71073 \text{ \AA}$
$b = 14.6482 (4) \text{ \AA}$	Cell parameters from 32862 reflections
$c = 14.6547 (4) \text{ \AA}$	$\theta = 2.9\text{--}27.5^\circ$
$\alpha = 100.745 (1)^\circ$	$\mu = 0.14 \text{ mm}^{-1}$
$\beta = 93.830 (2)^\circ$	$T = 120 \text{ K}$
$\gamma = 98.497 (2)^\circ$	Plate, colourless
$V = 2084.41 (9) \text{ \AA}^3$	$0.42 \times 0.05 \times 0.03 \text{ mm}$

Data collection

Bruker–Nonius Roper CCD camera on κ -goniostat diffractometer	$T_{\min} = 0.849$, $T_{\max} = 1.000$ 42885 measured reflections 9543 independent reflections 6505 reflections with $I > 2\sigma(I)$
Radiation source: Bruker–Nonius FR591 rotating anode	$R_{\text{int}} = 0.085$
Graphite monochromator	$\theta_{\max} = 27.6^\circ$, $\theta_{\min} = 2.9^\circ$
Detector resolution: 9.091 pixels mm^{-1}	$h = -12 \rightarrow 13$
φ & ω scans	$k = -18 \rightarrow 19$
Absorption correction: multi-scan (<i>SADABS</i> ; Sheldrick, 2007)	$l = -19 \rightarrow 19$

Refinement

Refinement on F^2	590 parameters
Least-squares matrix: full	7 restraints
$R[F^2 > 2\sigma(F^2)] = 0.074$	Primary atom site location: structure-invariant direct methods
$wR(F^2) = 0.180$	Secondary atom site location: difference Fourier map
$S = 1.04$	
9543 reflections	

Hydrogen site location: mixed
H atoms treated by a mixture of independent
and constrained refinement

$$w = 1/[\sigma^2(F_o^2) + (0.0525P)^2 + 4.9226P]$$

$$\text{where } P = (F_o^2 + 2F_c^2)/3$$

$$(\Delta/\sigma)_{\max} < 0.001$$

$$\Delta\rho_{\max} = 0.60 \text{ e \AA}^{-3}$$

$$\Delta\rho_{\min} = -0.58 \text{ e \AA}^{-3}$$

Special details

Geometry. All esds (except the esd in the dihedral angle between two l.s. planes) are estimated using the full covariance matrix. The cell esds are taken into account individually in the estimation of esds in distances, angles and torsion angles; correlations between esds in cell parameters are only used when they are defined by crystal symmetry. An approximate (isotropic) treatment of cell esds is used for estimating esds involving l.s. planes.

Refinement. Owing to poor agreement, possibly to interference from the beam-stop, one reflection, i.e. (0 -1 2), was omitted from the final cycles of refinement.

Fractional atomic coordinates and isotropic or equivalent isotropic displacement parameters (\AA^2)

	<i>x</i>	<i>y</i>	<i>z</i>	$U_{\text{iso}}^*/U_{\text{eq}}$
F1	0.2808 (2)	0.67260 (18)	0.16134 (18)	0.0504 (7)
F2	0.2712 (2)	0.65790 (19)	0.01402 (19)	0.0506 (7)
F3	0.2412 (2)	0.53596 (15)	0.07419 (19)	0.0430 (6)
F4	-0.1087 (2)	0.38548 (14)	0.16771 (16)	0.0344 (5)
F5	-0.03229 (19)	0.48942 (14)	0.29119 (15)	0.0319 (5)
F6	-0.2296 (2)	0.40671 (14)	0.28320 (16)	0.0364 (5)
O1	-0.0896 (2)	0.82971 (15)	-0.04003 (16)	0.0212 (5)
H1O	-0.061 (4)	0.869 (2)	0.0096 (16)	0.032*
N1	-0.0028 (2)	0.57189 (18)	0.12924 (19)	0.0207 (6)
N2	-0.3489 (3)	0.78367 (18)	-0.13680 (19)	0.0190 (5)
H1N	-0.289 (3)	0.8273 (18)	-0.152 (2)	0.023*
H2N	-0.390 (3)	0.811 (2)	-0.0906 (17)	0.023*
C1	0.0642 (3)	0.6271 (2)	0.0803 (2)	0.0198 (6)
C2	0.0089 (3)	0.6897 (2)	0.0331 (2)	0.0190 (6)
H2	0.0631	0.7264	-0.0019	0.023*
C3	-0.1251 (3)	0.6968 (2)	0.0384 (2)	0.0188 (6)
C4	-0.2021 (3)	0.6417 (2)	0.0930 (2)	0.0181 (6)
C5	-0.3393 (3)	0.6472 (2)	0.1083 (2)	0.0223 (7)
H5	-0.3852	0.6885	0.0799	0.027*
C6	-0.4056 (3)	0.5940 (2)	0.1630 (2)	0.0237 (7)
H6	-0.4971	0.5989	0.1728	0.028*
C7	-0.3403 (3)	0.5318 (2)	0.2053 (3)	0.0260 (7)
H7	-0.3881	0.4952	0.2435	0.031*
C8	-0.2090 (3)	0.5233 (2)	0.1922 (2)	0.0217 (7)
C9	-0.1351 (3)	0.5793 (2)	0.1366 (2)	0.0195 (6)
C10	0.2142 (3)	0.6225 (2)	0.0822 (2)	0.0244 (7)
C11	-0.1435 (3)	0.4521 (2)	0.2331 (3)	0.0259 (7)
C12	-0.1883 (3)	0.7644 (2)	-0.0125 (2)	0.0184 (6)
H12	-0.2441	0.8000	0.0309	0.022*
C13	-0.2802 (3)	0.7122 (2)	-0.1001 (2)	0.0176 (6)
H13	-0.3506	0.6652	-0.0815	0.021*
C14	-0.4440 (3)	0.7429 (2)	-0.2226 (2)	0.0263 (7)

H14A	-0.4816	0.7940	-0.2457	0.032*
H14B	-0.5202	0.6991	-0.2071	0.032*
C15	-0.3715 (4)	0.6904 (3)	-0.2983 (2)	0.0295 (8)
H15A	-0.3033	0.7359	-0.3196	0.035*
H15B	-0.4376	0.6596	-0.3524	0.035*
C16	-0.3015 (3)	0.6160 (2)	-0.2630 (2)	0.0262 (7)
H16A	-0.3704	0.5665	-0.2484	0.031*
H16B	-0.2501	0.5861	-0.3123	0.031*
C17	-0.2054 (3)	0.6606 (2)	-0.1756 (2)	0.0201 (6)
H17A	-0.1649	0.6110	-0.1517	0.024*
H17B	-0.1312	0.7056	-0.1918	0.024*
F7	-0.6032 (3)	0.6297 (2)	0.3672 (3)	0.0874 (12)
F8	-0.6420 (2)	0.7695 (2)	0.3979 (2)	0.0572 (8)
F9	-0.5432 (2)	0.7145 (2)	0.50201 (19)	0.0670 (9)
F10	-0.1334 (2)	0.67918 (15)	0.55849 (15)	0.0343 (5)
F11	-0.1959 (2)	0.55632 (14)	0.44945 (16)	0.0371 (5)
F12	0.0147 (2)	0.60063 (14)	0.49868 (15)	0.0332 (5)
O2	-0.4008 (2)	0.92583 (16)	0.18909 (16)	0.0236 (5)
H2O	-0.424 (4)	0.897 (2)	0.1338 (12)	0.035*
N3	-0.3160 (3)	0.71100 (19)	0.4089 (2)	0.0229 (6)
N4	-0.1656 (3)	1.06682 (18)	0.20532 (19)	0.0186 (5)
H3N	-0.240 (2)	1.071 (2)	0.172 (2)	0.022*
H4N	-0.114 (3)	1.036 (2)	0.168 (2)	0.022*
C18	-0.4157 (3)	0.7498 (2)	0.3795 (2)	0.0239 (7)
C19	-0.4077 (3)	0.8153 (2)	0.3206 (2)	0.0221 (7)
H19	-0.4848	0.8413	0.3036	0.027*
C20	-0.2853 (3)	0.8408 (2)	0.2883 (2)	0.0188 (6)
C21	-0.1731 (3)	0.7995 (2)	0.3149 (2)	0.0188 (6)
C22	-0.0438 (3)	0.8172 (2)	0.2819 (2)	0.0191 (6)
H22	-0.0287	0.8594	0.2402	0.023*
C23	0.0591 (3)	0.7740 (2)	0.3097 (2)	0.0229 (7)
H23	0.1448	0.7858	0.2864	0.027*
C24	0.0399 (3)	0.7124 (2)	0.3722 (2)	0.0224 (7)
H24	0.1126	0.6831	0.3907	0.027*
C25	-0.0821 (3)	0.6942 (2)	0.4067 (2)	0.0223 (7)
C26	-0.1939 (3)	0.7360 (2)	0.3771 (2)	0.0191 (6)
C27	-0.5505 (3)	0.7155 (3)	0.4130 (3)	0.0339 (8)
C28	-0.1002 (3)	0.6326 (2)	0.4778 (2)	0.0259 (7)
C29	-0.2730 (3)	0.9119 (2)	0.2244 (2)	0.0182 (6)
H29	-0.2221	0.8882	0.1710	0.022*
C30	-0.1964 (3)	1.0076 (2)	0.2770 (2)	0.0187 (6)
H30	-0.1091	0.9978	0.3076	0.022*
C31	-0.0944 (3)	1.1651 (2)	0.2457 (2)	0.0243 (7)
H31A	-0.0841	1.2015	0.1953	0.029*
H31B	-0.0029	1.1628	0.2739	0.029*
C32	-0.1729 (3)	1.2135 (2)	0.3186 (3)	0.0291 (8)
H32A	-0.2611	1.2213	0.2891	0.035*
H32B	-0.1223	1.2768	0.3467	0.035*

C33	-0.1966 (4)	1.1559 (2)	0.3949 (3)	0.0309 (8)
H33A	-0.1087	1.1505	0.4265	0.037*
H33B	-0.2494	1.1880	0.4420	0.037*
C34	-0.2739 (3)	1.0578 (2)	0.3511 (2)	0.0253 (7)
H34A	-0.2880	1.0202	0.4002	0.030*
H34B	-0.3638	1.0634	0.3226	0.030*
O3	0.3721 (2)	0.87780 (16)	-0.09688 (16)	0.0245 (5)
O4	0.5232 (2)	0.85378 (16)	0.00986 (16)	0.0246 (5)
O5	0.1931 (2)	1.05633 (15)	0.18195 (15)	0.0217 (5)
O6	0.0086 (2)	0.96016 (15)	0.10987 (16)	0.0215 (5)
C35	0.4142 (3)	0.8829 (2)	-0.0146 (2)	0.0194 (6)
C36	0.3374 (3)	0.9243 (2)	0.0649 (2)	0.0212 (6)
H36A	0.3096	0.8752	0.1011	0.025*
H36B	0.3993	0.9762	0.1072	0.025*
C37	0.2127 (3)	0.9620 (2)	0.0338 (2)	0.0188 (6)
H37A	0.2407	1.0150	0.0024	0.023*
H37B	0.1535	0.9118	-0.0123	0.023*
C38	0.1328 (3)	0.9955 (2)	0.1142 (2)	0.0176 (6)
O7	0.1253 (3)	1.0539 (3)	0.3588 (2)	0.0587 (9)
H7O	0.147 (6)	1.052 (4)	0.3036 (17)	0.088*
C39	0.2349 (6)	1.0663 (5)	0.4209 (4)	0.083 (2)
H39A	0.2025	1.0473	0.4780	0.100*
H39B	0.2682	1.1349	0.4375	0.100*
C40	0.3465 (6)	1.0231 (7)	0.4013 (4)	0.105 (3)
H40A	0.3264	0.9569	0.4070	0.158*
H40B	0.4242	1.0552	0.4456	0.158*
H40C	0.3679	1.0265	0.3377	0.158*

Atomic displacement parameters (\AA^2)

	U^{11}	U^{22}	U^{33}	U^{12}	U^{13}	U^{23}
F1	0.0210 (11)	0.0686 (16)	0.0492 (15)	0.0145 (10)	-0.0092 (10)	-0.0207 (13)
F2	0.0212 (11)	0.0813 (18)	0.0645 (17)	0.0170 (11)	0.0168 (10)	0.0419 (15)
F3	0.0250 (11)	0.0294 (11)	0.0778 (18)	0.0147 (9)	0.0100 (11)	0.0087 (11)
F4	0.0393 (12)	0.0239 (10)	0.0413 (13)	0.0132 (8)	0.0039 (9)	0.0037 (9)
F5	0.0298 (11)	0.0327 (11)	0.0343 (12)	0.0066 (8)	-0.0040 (9)	0.0112 (9)
F6	0.0360 (11)	0.0318 (11)	0.0482 (14)	0.0061 (9)	0.0097 (10)	0.0225 (10)
O1	0.0189 (11)	0.0214 (11)	0.0216 (13)	0.0002 (8)	-0.0014 (9)	0.0033 (9)
N1	0.0161 (12)	0.0221 (13)	0.0230 (15)	0.0049 (10)	-0.0009 (10)	0.0016 (11)
N2	0.0162 (13)	0.0197 (13)	0.0201 (15)	0.0033 (10)	-0.0002 (10)	0.0017 (11)
C1	0.0158 (14)	0.0208 (15)	0.0208 (17)	0.0049 (11)	-0.0011 (12)	-0.0011 (13)
C2	0.0147 (14)	0.0213 (15)	0.0200 (17)	0.0024 (11)	0.0014 (11)	0.0027 (13)
C3	0.0202 (15)	0.0163 (14)	0.0193 (17)	0.0047 (11)	-0.0001 (12)	0.0017 (12)
C4	0.0139 (14)	0.0192 (15)	0.0195 (17)	0.0027 (11)	-0.0001 (11)	0.0002 (12)
C5	0.0183 (15)	0.0226 (16)	0.0259 (18)	0.0063 (12)	0.0009 (12)	0.0025 (14)
C6	0.0125 (14)	0.0267 (16)	0.0312 (19)	0.0030 (12)	0.0026 (12)	0.0043 (14)
C7	0.0192 (16)	0.0276 (17)	0.032 (2)	0.0017 (13)	0.0030 (13)	0.0078 (15)
C8	0.0211 (15)	0.0187 (15)	0.0241 (18)	0.0036 (12)	-0.0007 (12)	0.0021 (13)

C9	0.0189 (15)	0.0173 (14)	0.0216 (17)	0.0049 (11)	0.0002 (12)	0.0010 (12)
C10	0.0178 (15)	0.0251 (16)	0.0297 (19)	0.0058 (12)	-0.0008 (13)	0.0036 (14)
C11	0.0230 (16)	0.0239 (16)	0.031 (2)	0.0034 (13)	0.0022 (14)	0.0075 (15)
C12	0.0127 (14)	0.0198 (15)	0.0229 (17)	0.0040 (11)	0.0000 (11)	0.0047 (13)
C13	0.0156 (14)	0.0219 (15)	0.0165 (16)	0.0045 (11)	0.0022 (11)	0.0052 (12)
C14	0.0243 (16)	0.0326 (18)	0.0203 (18)	0.0088 (13)	-0.0045 (13)	0.0002 (14)
C15	0.0336 (19)	0.0365 (19)	0.0172 (18)	0.0116 (15)	-0.0039 (14)	0.0003 (15)
C16	0.0264 (17)	0.0268 (17)	0.0230 (19)	0.0041 (13)	0.0033 (13)	-0.0013 (14)
C17	0.0205 (15)	0.0176 (15)	0.0228 (18)	0.0039 (11)	0.0038 (12)	0.0045 (13)
F7	0.0547 (18)	0.0618 (19)	0.127 (3)	-0.0282 (14)	0.0462 (19)	-0.0129 (19)
F8	0.0204 (11)	0.098 (2)	0.0746 (19)	0.0233 (12)	0.0199 (11)	0.0562 (17)
F9	0.0271 (12)	0.144 (3)	0.0493 (17)	0.0202 (14)	0.0152 (11)	0.0595 (19)
F10	0.0382 (12)	0.0429 (12)	0.0272 (12)	0.0135 (9)	0.0061 (9)	0.0139 (10)
F11	0.0348 (12)	0.0283 (11)	0.0494 (14)	-0.0020 (9)	0.0005 (10)	0.0177 (10)
F12	0.0325 (11)	0.0342 (11)	0.0385 (13)	0.0146 (9)	-0.0008 (9)	0.0159 (10)
O2	0.0196 (11)	0.0317 (13)	0.0199 (13)	0.0086 (9)	-0.0029 (9)	0.0047 (10)
N3	0.0180 (13)	0.0271 (14)	0.0257 (16)	0.0047 (10)	0.0039 (11)	0.0090 (12)
N4	0.0184 (13)	0.0221 (13)	0.0167 (14)	0.0072 (10)	0.0028 (10)	0.0046 (11)
C18	0.0174 (15)	0.0301 (17)	0.0241 (18)	0.0027 (12)	0.0015 (12)	0.0058 (14)
C19	0.0144 (14)	0.0258 (16)	0.0272 (19)	0.0059 (12)	0.0034 (12)	0.0053 (14)
C20	0.0171 (14)	0.0190 (15)	0.0186 (17)	0.0019 (11)	-0.0005 (11)	0.0006 (12)
C21	0.0143 (14)	0.0207 (15)	0.0198 (17)	0.0015 (11)	-0.0004 (11)	0.0021 (13)
C22	0.0184 (15)	0.0215 (15)	0.0172 (16)	0.0033 (11)	0.0008 (11)	0.0034 (12)
C23	0.0138 (14)	0.0256 (16)	0.0281 (19)	0.0037 (12)	0.0014 (12)	0.0024 (14)
C24	0.0211 (15)	0.0201 (15)	0.0252 (18)	0.0057 (12)	-0.0020 (12)	0.0023 (13)
C25	0.0219 (15)	0.0207 (15)	0.0232 (18)	0.0026 (12)	-0.0024 (12)	0.0041 (13)
C26	0.0187 (15)	0.0184 (14)	0.0185 (17)	0.0024 (11)	-0.0009 (12)	0.0007 (12)
C27	0.0206 (17)	0.044 (2)	0.039 (2)	0.0029 (15)	0.0051 (15)	0.0150 (18)
C28	0.0248 (17)	0.0272 (17)	0.0271 (19)	0.0069 (13)	0.0003 (13)	0.0079 (15)
C29	0.0141 (14)	0.0211 (15)	0.0196 (17)	0.0051 (11)	0.0009 (11)	0.0030 (13)
C30	0.0179 (14)	0.0226 (15)	0.0160 (16)	0.0057 (11)	0.0026 (11)	0.0026 (12)
C31	0.0212 (16)	0.0232 (16)	0.0284 (19)	0.0010 (12)	-0.0007 (13)	0.0080 (14)
C32	0.0265 (17)	0.0225 (16)	0.036 (2)	0.0081 (13)	-0.0040 (14)	-0.0009 (15)
C33	0.040 (2)	0.0285 (18)	0.0228 (19)	0.0104 (15)	0.0041 (15)	-0.0023 (15)
C34	0.0284 (17)	0.0270 (17)	0.0219 (18)	0.0071 (13)	0.0099 (13)	0.0041 (14)
O3	0.0218 (11)	0.0347 (13)	0.0185 (13)	0.0113 (9)	0.0004 (9)	0.0046 (10)
O4	0.0181 (11)	0.0343 (13)	0.0224 (13)	0.0115 (9)	-0.0002 (9)	0.0033 (10)
O5	0.0206 (11)	0.0249 (11)	0.0186 (12)	0.0031 (9)	0.0006 (9)	0.0023 (9)
O6	0.0150 (10)	0.0225 (11)	0.0261 (13)	0.0024 (8)	0.0035 (9)	0.0027 (9)
C35	0.0149 (14)	0.0185 (15)	0.0261 (18)	0.0035 (11)	0.0024 (12)	0.0071 (13)
C36	0.0194 (15)	0.0266 (16)	0.0194 (17)	0.0082 (12)	0.0030 (12)	0.0056 (13)
C37	0.0146 (14)	0.0222 (15)	0.0193 (17)	0.0042 (11)	0.0012 (11)	0.0028 (13)
C38	0.0170 (14)	0.0190 (15)	0.0189 (17)	0.0068 (11)	0.0015 (11)	0.0061 (12)
O7	0.0374 (16)	0.111 (3)	0.0352 (18)	0.0244 (17)	0.0060 (13)	0.0237 (19)
C39	0.074 (4)	0.136 (6)	0.040 (3)	0.053 (4)	-0.015 (3)	-0.004 (3)
C40	0.052 (3)	0.220 (9)	0.058 (4)	0.060 (4)	0.004 (3)	0.036 (5)

Geometric parameters (\AA , $^{\circ}$)

F1—C10	1.328 (4)	N4—C31	1.502 (4)
F2—C10	1.333 (4)	N4—C30	1.502 (4)
F3—C10	1.321 (4)	N4—H3N	0.882 (10)
F4—C11	1.338 (4)	N4—H4N	0.882 (10)
F5—C11	1.338 (4)	C18—C19	1.403 (5)
F6—C11	1.352 (4)	C18—C27	1.518 (5)
O1—C12	1.406 (4)	C19—C20	1.373 (4)
O1—H1O	0.840 (10)	C19—H19	0.9500
N1—C1	1.319 (4)	C20—C21	1.419 (4)
N1—C9	1.358 (4)	C20—C29	1.522 (4)
N2—C13	1.495 (4)	C21—C22	1.421 (4)
N2—C14	1.497 (4)	C21—C26	1.423 (4)
N2—H1N	0.880 (10)	C22—C23	1.366 (4)
N2—H2N	0.883 (10)	C22—H22	0.9500
C1—C2	1.401 (4)	C23—C24	1.404 (5)
C1—C10	1.517 (4)	C23—H23	0.9500
C2—C3	1.370 (4)	C24—C25	1.365 (5)
C2—H2	0.9500	C24—H24	0.9500
C3—C4	1.425 (4)	C25—C26	1.435 (4)
C3—C12	1.530 (4)	C25—C28	1.504 (5)
C4—C5	1.422 (4)	C29—C30	1.533 (4)
C4—C9	1.428 (4)	C29—H29	1.0000
C5—C6	1.357 (5)	C30—C34	1.519 (4)
C5—H5	0.9500	C30—H30	1.0000
C6—C7	1.406 (5)	C31—C32	1.504 (5)
C6—H6	0.9500	C31—H31A	0.9900
C7—C8	1.365 (4)	C31—H31B	0.9900
C7—H7	0.9500	C32—C33	1.532 (5)
C8—C9	1.427 (4)	C32—H32A	0.9900
C8—C11	1.503 (4)	C32—H32B	0.9900
C12—C13	1.533 (4)	C33—C34	1.529 (5)
C12—H12	1.0000	C33—H33A	0.9900
C13—C17	1.525 (4)	C33—H33B	0.9900
C13—H13	1.0000	C34—H34A	0.9900
C14—C15	1.519 (5)	C34—H34B	0.9900
C14—H14A	0.9900	O3—C35	1.236 (4)
C14—H14B	0.9900	O4—C35	1.285 (4)
C15—C16	1.529 (5)	O5—C38	1.255 (4)
C15—H15A	0.9900	O6—C38	1.271 (4)
C15—H15B	0.9900	C35—C36	1.522 (4)
C16—C17	1.527 (5)	C36—C37	1.517 (4)
C16—H16A	0.9900	C36—H36A	0.9900
C16—H16B	0.9900	C36—H36B	0.9900
C17—H17A	0.9900	C37—C38	1.517 (4)
C17—H17B	0.9900	C37—H37A	0.9900
F7—C27	1.323 (5)	C37—H37B	0.9900

F8—C27	1.331 (4)	O7—C39	1.347 (6)
F9—C27	1.304 (5)	O7—H7O	0.847 (10)
F10—C28	1.340 (4)	C39—C40	1.388 (8)
F11—C28	1.341 (4)	C39—H39A	0.9900
F12—C28	1.346 (4)	C39—H39B	0.9900
O2—C29	1.409 (3)	C40—H40A	0.9800
O2—H2O	0.841 (10)	C40—H40B	0.9800
N3—C18	1.309 (4)	C40—H40C	0.9800
N3—C26	1.363 (4)		
C12—O1—H1O	104 (3)	C21—C20—C29	121.6 (3)
C1—N1—C9	116.7 (3)	C22—C21—C20	123.7 (3)
C13—N2—C14	113.4 (2)	C22—C21—C26	119.0 (3)
C13—N2—H1N	111 (2)	C20—C21—C26	117.3 (3)
C14—N2—H1N	106 (2)	C23—C22—C21	120.4 (3)
C13—N2—H2N	106 (2)	C23—C22—H22	119.8
C14—N2—H2N	112 (2)	C21—C22—H22	119.8
H1N—N2—H2N	108 (3)	C22—C23—C24	120.8 (3)
N1—C1—C2	125.4 (3)	C22—C23—H23	119.6
N1—C1—C10	114.3 (3)	C24—C23—H23	119.6
C2—C1—C10	120.2 (3)	C25—C24—C23	120.8 (3)
C3—C2—C1	118.6 (3)	C25—C24—H24	119.6
C3—C2—H2	120.7	C23—C24—H24	119.6
C1—C2—H2	120.7	C24—C25—C26	120.1 (3)
C2—C3—C4	118.9 (3)	C24—C25—C28	120.7 (3)
C2—C3—C12	119.8 (3)	C26—C25—C28	119.2 (3)
C4—C3—C12	121.3 (3)	N3—C26—C21	123.3 (3)
C5—C4—C3	124.0 (3)	N3—C26—C25	117.9 (3)
C5—C4—C9	118.7 (3)	C21—C26—C25	118.8 (3)
C3—C4—C9	117.3 (3)	F9—C27—F7	107.9 (3)
C6—C5—C4	120.8 (3)	F9—C27—F8	106.4 (3)
C6—C5—H5	119.6	F7—C27—F8	105.4 (3)
C4—C5—H5	119.6	F9—C27—C18	113.5 (3)
C5—C6—C7	120.7 (3)	F7—C27—C18	111.5 (3)
C5—C6—H6	119.7	F8—C27—C18	111.6 (3)
C7—C6—H6	119.7	F10—C28—F11	107.0 (3)
C8—C7—C6	120.8 (3)	F10—C28—F12	106.1 (3)
C8—C7—H7	119.6	F11—C28—F12	106.4 (3)
C6—C7—H7	119.6	F10—C28—C25	112.0 (3)
C7—C8—C9	120.1 (3)	F11—C28—C25	113.4 (3)
C7—C8—C11	120.1 (3)	F12—C28—C25	111.4 (3)
C9—C8—C11	119.7 (3)	O2—C29—C20	111.7 (2)
N1—C9—C8	118.1 (3)	O2—C29—C30	107.7 (2)
N1—C9—C4	123.0 (3)	C20—C29—C30	110.8 (3)
C8—C9—C4	118.8 (3)	O2—C29—H29	108.9
F3—C10—F1	107.1 (3)	C20—C29—H29	108.9
F3—C10—F2	106.5 (3)	C30—C29—H29	108.9
F1—C10—F2	105.9 (3)	N4—C30—C34	110.2 (2)

F3—C10—C1	113.2 (3)	N4—C30—C29	106.9 (2)
F1—C10—C1	111.1 (3)	C34—C30—C29	113.9 (3)
F2—C10—C1	112.5 (3)	N4—C30—H30	108.6
F5—C11—F4	107.0 (3)	C34—C30—H30	108.6
F5—C11—F6	106.0 (3)	C29—C30—H30	108.6
F4—C11—F6	106.2 (3)	N4—C31—C32	110.6 (3)
F5—C11—C8	114.0 (3)	N4—C31—H31A	109.5
F4—C11—C8	112.6 (3)	C32—C31—H31A	109.5
F6—C11—C8	110.6 (3)	N4—C31—H31B	109.5
O1—C12—C3	112.0 (2)	C32—C31—H31B	109.5
O1—C12—C13	107.7 (2)	H31A—C31—H31B	108.1
C3—C12—C13	112.0 (2)	C31—C32—C33	110.5 (3)
O1—C12—H12	108.4	C31—C32—H32A	109.5
C3—C12—H12	108.4	C33—C32—H32A	109.5
C13—C12—H12	108.4	C31—C32—H32B	109.5
N2—C13—C17	110.2 (2)	C33—C32—H32B	109.5
N2—C13—C12	107.1 (2)	H32A—C32—H32B	108.1
C17—C13—C12	113.9 (2)	C34—C33—C32	109.4 (3)
N2—C13—H13	108.5	C34—C33—H33A	109.8
C17—C13—H13	108.5	C32—C33—H33A	109.8
C12—C13—H13	108.5	C34—C33—H33B	109.8
N2—C14—C15	110.6 (3)	C32—C33—H33B	109.8
N2—C14—H14A	109.5	H33A—C33—H33B	108.2
C15—C14—H14A	109.5	C30—C34—C33	110.9 (3)
N2—C14—H14B	109.5	C30—C34—H34A	109.5
C15—C14—H14B	109.5	C33—C34—H34A	109.5
H14A—C14—H14B	108.1	C30—C34—H34B	109.5
C14—C15—C16	111.4 (3)	C33—C34—H34B	109.5
C14—C15—H15A	109.4	H34A—C34—H34B	108.0
C16—C15—H15A	109.4	O3—C35—O4	123.2 (3)
C14—C15—H15B	109.4	O3—C35—C36	121.1 (3)
C16—C15—H15B	109.4	O4—C35—C36	115.7 (3)
H15A—C15—H15B	108.0	C37—C36—C35	114.3 (3)
C17—C16—C15	110.5 (3)	C37—C36—H36A	108.7
C17—C16—H16A	109.5	C35—C36—H36A	108.7
C15—C16—H16A	109.5	C37—C36—H36B	108.7
C17—C16—H16B	109.5	C35—C36—H36B	108.7
C15—C16—H16B	109.5	H36A—C36—H36B	107.6
H16A—C16—H16B	108.1	C38—C37—C36	112.7 (3)
C13—C17—C16	110.9 (2)	C38—C37—H37A	109.1
C13—C17—H17A	109.5	C36—C37—H37A	109.1
C16—C17—H17A	109.5	C38—C37—H37B	109.1
C13—C17—H17B	109.5	C36—C37—H37B	109.1
C16—C17—H17B	109.5	H37A—C37—H37B	107.8
H17A—C17—H17B	108.1	O5—C38—O6	123.4 (3)
C29—O2—H2O	113 (3)	O5—C38—C37	118.3 (3)
C18—N3—C26	116.1 (3)	O6—C38—C37	118.3 (3)
C31—N4—C30	114.0 (2)	C39—O7—H7O	112 (4)

C31—N4—H3N	108 (2)	O7—C39—C40	122.4 (5)
C30—N4—H3N	111 (2)	O7—C39—H39A	106.7
C31—N4—H4N	111 (2)	C40—C39—H39A	106.7
C30—N4—H4N	105 (2)	O7—C39—H39B	106.7
H3N—N4—H4N	108 (3)	C40—C39—H39B	106.7
N3—C18—C19	126.2 (3)	H39A—C39—H39B	106.6
N3—C18—C27	113.7 (3)	C39—C40—H40A	109.5
C19—C18—C27	120.0 (3)	C39—C40—H40B	109.5
C20—C19—C18	118.0 (3)	H40A—C40—H40B	109.5
C20—C19—H19	121.0	C39—C40—H40C	109.5
C18—C19—H19	121.0	H40A—C40—H40C	109.5
C19—C20—C21	119.0 (3)	H40B—C40—H40C	109.5
C19—C20—C29	119.4 (3)		
C9—N1—C1—C2	−2.4 (5)	C27—C18—C19—C20	−176.8 (3)
C9—N1—C1—C10	174.4 (3)	C18—C19—C20—C21	0.5 (5)
N1—C1—C2—C3	1.3 (5)	C18—C19—C20—C29	−179.9 (3)
C10—C1—C2—C3	−175.4 (3)	C19—C20—C21—C22	176.8 (3)
C1—C2—C3—C4	1.1 (4)	C29—C20—C21—C22	−2.9 (5)
C1—C2—C3—C12	−179.9 (3)	C19—C20—C21—C26	−2.2 (4)
C2—C3—C4—C5	176.1 (3)	C29—C20—C21—C26	178.1 (3)
C12—C3—C4—C5	−2.8 (5)	C20—C21—C22—C23	−179.1 (3)
C2—C3—C4—C9	−2.1 (4)	C26—C21—C22—C23	−0.2 (5)
C12—C3—C4—C9	178.9 (3)	C21—C22—C23—C24	−0.9 (5)
C3—C4—C5—C6	−178.4 (3)	C22—C23—C24—C25	0.1 (5)
C9—C4—C5—C6	−0.2 (5)	C23—C24—C25—C26	1.8 (5)
C4—C5—C6—C7	−0.4 (5)	C23—C24—C25—C28	−176.5 (3)
C5—C6—C7—C8	−0.1 (5)	C18—N3—C26—C21	−0.7 (5)
C6—C7—C8—C9	1.3 (5)	C18—N3—C26—C25	−179.2 (3)
C6—C7—C8—C11	−176.2 (3)	C22—C21—C26—N3	−176.6 (3)
C1—N1—C9—C8	−177.5 (3)	C20—C21—C26—N3	2.4 (5)
C1—N1—C9—C4	1.2 (5)	C22—C21—C26—C25	1.9 (4)
C7—C8—C9—N1	176.8 (3)	C20—C21—C26—C25	−179.0 (3)
C11—C8—C9—N1	−5.6 (5)	C24—C25—C26—N3	175.9 (3)
C7—C8—C9—C4	−2.0 (5)	C28—C25—C26—N3	−5.8 (4)
C11—C8—C9—C4	175.6 (3)	C24—C25—C26—C21	−2.7 (5)
C5—C4—C9—N1	−177.3 (3)	C28—C25—C26—C21	175.5 (3)
C3—C4—C9—N1	1.0 (5)	N3—C18—C27—F9	47.0 (5)
C5—C4—C9—C8	1.4 (4)	C19—C18—C27—F9	−134.4 (4)
C3—C4—C9—C8	179.7 (3)	N3—C18—C27—F7	−75.0 (4)
N1—C1—C10—F3	42.1 (4)	C19—C18—C27—F7	103.5 (4)
C2—C1—C10—F3	−140.9 (3)	N3—C18—C27—F8	167.3 (3)
N1—C1—C10—F1	−78.4 (4)	C19—C18—C27—F8	−14.2 (5)
C2—C1—C10—F1	98.6 (4)	C24—C25—C28—F10	118.1 (3)
N1—C1—C10—F2	163.0 (3)	C26—C25—C28—F10	−60.2 (4)
C2—C1—C10—F2	−20.0 (4)	C24—C25—C28—F11	−120.7 (3)
C7—C8—C11—F5	−121.8 (3)	C26—C25—C28—F11	61.1 (4)
C9—C8—C11—F5	60.6 (4)	C24—C25—C28—F12	−0.6 (4)

C7—C8—C11—F4	116.1 (3)	C26—C25—C28—F12	-178.9 (3)
C9—C8—C11—F4	-61.5 (4)	C19—C20—C29—O2	-14.1 (4)
C7—C8—C11—F6	-2.5 (5)	C21—C20—C29—O2	165.5 (3)
C9—C8—C11—F6	179.9 (3)	C19—C20—C29—C30	105.9 (3)
C2—C3—C12—O1	-15.4 (4)	C21—C20—C29—C30	-74.4 (4)
C4—C3—C12—O1	163.5 (3)	C31—N4—C30—C34	53.7 (3)
C2—C3—C12—C13	105.7 (3)	C31—N4—C30—C29	177.9 (2)
C4—C3—C12—C13	-75.4 (4)	O2—C29—C30—N4	-68.4 (3)
C14—N2—C13—C17	56.2 (3)	C20—C29—C30—N4	169.2 (2)
C14—N2—C13—C12	-179.4 (2)	O2—C29—C30—C34	53.6 (3)
O1—C12—C13—N2	-63.4 (3)	C20—C29—C30—C34	-68.9 (3)
C3—C12—C13—N2	173.1 (2)	C30—N4—C31—C32	-54.6 (3)
O1—C12—C13—C17	58.7 (3)	N4—C31—C32—C33	56.3 (4)
C3—C12—C13—C17	-64.8 (3)	C31—C32—C33—C34	-58.7 (4)
C13—N2—C14—C15	-55.5 (4)	N4—C30—C34—C33	-55.2 (4)
N2—C14—C15—C16	54.4 (4)	C29—C30—C34—C33	-175.3 (3)
C14—C15—C16—C17	-55.4 (4)	C32—C33—C34—C30	58.3 (4)
N2—C13—C17—C16	-55.8 (3)	O3—C35—C36—C37	-3.0 (4)
C12—C13—C17—C16	-176.1 (3)	O4—C35—C36—C37	177.4 (3)
C15—C16—C17—C13	56.0 (3)	C35—C36—C37—C38	175.4 (3)
C26—N3—C18—C19	-1.4 (5)	C36—C37—C38—O5	55.5 (4)
C26—N3—C18—C27	177.0 (3)	C36—C37—C38—O6	-124.1 (3)
N3—C18—C19—C20	1.5 (5)		

Hydrogen-bond geometry (Å, °)

Cg1 is the centroid of the (N1,C1—C4,C9) ring.

D—H···A	D—H	H···A	D···A	D—H···A
N2—H1N···O1	0.88 (3)	2.49 (3)	2.806 (4)	102 (2)
N4—H3N···O2	0.88 (2)	2.54 (3)	2.863 (4)	103 (2)
O1—H1O···O6	0.84 (3)	1.81 (3)	2.653 (3)	175 (2)
O2—H2O···O4 ⁱ	0.84 (2)	1.82 (2)	2.656 (3)	170 (3)
N2—H1N···O5 ⁱⁱ	0.88 (3)	1.97 (3)	2.830 (4)	165 (3)
N2—H2N···O4 ⁱ	0.88 (3)	1.82 (3)	2.694 (4)	173 (3)
N4—H3N···O3 ⁱⁱ	0.88 (2)	1.99 (3)	2.832 (4)	161 (3)
N4—H4N···O6	0.89 (3)	1.92 (3)	2.789 (4)	168 (3)
O7—H7O···O5	0.85 (3)	1.88 (3)	2.729 (4)	176 (7)
C30—H30···O7	1.00	2.40	3.296 (4)	149
C10—F3···Cg1 ⁱⁱⁱ	1.32 (1)	3.28 (1)	4.101 (3)	120 (1)

Symmetry codes: (i) $x-1, y, z$; (ii) $-x, -y+2, -z$; (iii) $-x, -y+1, -z$.